The effects of romosozumab combined with active vitamin D 3 on fracture healing in ovariectomized rats

Ryota Takase
Oita University Hospital Rehabilitation Center, Oita University
Yuta Tsubouchi
School of Physical Therapy, Faculty of Rehabilitation, Reiwa Health Sciences University
Takefumi Otsu
Division of Mechatronics, Department of Science and Engineering, Oita University
Takashi Kataoka
Oita University Hospital Rehabilitation Center, Oita University
Tatsuya Iwasaki
Department of Rehabilitation Medicine, Faculty of Medicine, Oita University
Masashi Kataoka (mkataoka@oita-u.ac.jp)
Physical Therapy Course of Study, Faculty of Welfare and Health Sciences, Oita University
Hiroshi Tsumura
Department of Orthopaedic Surgery, Faculty of Medicine, Oita University

Research Article

Keywords: Romosozumab, fracture healing, ovariectomized, active vitamin D3

Posted Date: June 22nd, 2022

DOI: https://doi.org/10.21203/rs.3.rs-1765445/v1

Abstract

Background: In this study, we investigated the potential acceleration of fracture healing and the bone mineral density-increasing effects of the combination therapy of romosozumab and active vitamin D_3 on fractures in ovariectomized rats.

Methods: Ovariectomy was performed on forty 24-week-old female Sprague–Dawley rats. After 8 weeks, the rats underwent removal of the periosteum and osteotomy of the femoral shaft followed by osteosynthesis with intramedullary nailing to create fracture models. After surgery, the 40 rats were divided into four groups: the C group (control), the R group (romosozumab, 25 mg/kg, once a month via subcutaneous injection), the VD group (active vitamin D_3, 0.2 μg/kg, twice a week via subcutaneous injection), and the R + VD group. A further 10 rats were prepared as the sham group. Ten weeks postintervention, both femurs were removed from all rats, and blood was collected. Soft X-ray imaging was used to evaluate bone union, and microcomputed tomography (micro-CT) was used for bone morphometric evaluation. Toluidine blue staining of undecalcified specimens was used for histopathological evaluation, and bone turnover marker levels were measured using enzyme-linked immunosorbent assay.

Results: Bone morphometry analysis by micro-CT revealed increased mineral density of the trabecular bone in rat femurs from the R + VD group, demonstrating the effectiveness of combination therapy with romosozumab plus active vitamin D_3. However, no differences in bone union evaluated using soft X-ray imaging were observed, demonstrating no acceleration of fracture healing.

Conclusions: Although combination therapy with romosozumab and active vitamin D_3 increased the trabecular bone volume, there was no evidence that it could accelerate fracture healing.

Background

The incidence of delayed union and nonunion is approximately 5% of all fractures[1][2], and after osteosynthesis, they occasionally cause considerable functional and socioeconomic problems for patients. These complications severely affect activities of daily living; therefore, achieving early bone union and returning patients to society are important issues to address[3][4].

Romosozumab is an antibody that targets sclerostin. It is useful for the treatment of osteoporosis, especially in elderly women with severe osteoporosis. Several reports have described the effect of romosozumab administration on the promotion of bone healing[5][6][7]. On the other hand romosozumab was found to increase the callus volume, but bone healing was not accelerated[8][9]. The acceleration of fracture healing after treatment with romosozumab combined with active vitamin D_3 in ovariectomized (OVX) rat fracture models has not yet been reported.

When administering romosozumab, active vitamin D_3 administration is recommended. Because reducing osteoclast activity can lead to hypocalcemia, the administration of active vitamin D_3 is essential. It

remains unknown whether active vitamin D_3 administration in an OVX fracture model is effective for fracture healing[10][11].

Previously, we reported that the combination of low-dose teriparatide and zoledronic acid promotes callus formation, increases callus volume, and enhances bone union in a rat model of refractory fractures[12].

For this study, we hypothesized that an excessive decrease in osteoclast activity after administration of romosozumab should result in the inhibition of endochondral ossification bone union in a fracture model, with the hypocalcemia associated with romosozumab administration producing an additional negative effect on bone fusion. To test this hypothesis, we investigated the promotion of the fracture healing effect via combination therapy with romosozumab and active vitamin D_3 in an OVX rat fracture model.

Methods

Surgical technique used to construct the ovariectomies and the femoral fracture model

Approval was obtained from Oita University's Animal Research Committee prior to animal experimentation (Oita University Institutional Animal Ethics Committee, no. 182402). Before the procedure, a total of 40 female Sprague–Dawley rats (24 weeks old; CLEA Japan, Inc., Tokyo, Japan) were anesthetized via intraperitoneal injection containing 0.3–0.4 ml of 0.15 mg/kg medetomidine + 2 mg/kg midazolam + 2.5 mg/kg butorphanol. All operations were conducted in a standard sterile environment. Rats underwent ovariectomy or sham surgery, raised for 8 weeks, and then underwent weight measurement to confirm weight gain. After 8 weeks, all rats underwent femoral osteotomy. The right hind limb was prepared for the operation. With the rats in the lateral position, the right femur was located using the posterolateral approach. The periosteum of the femur was circumferentially incised, elevated, and stripped. Subsequently, the femur at the osteotomy site was exposed. A transverse osteotomy was made with a sagittal saw (Stryker, Kalamazoo, MI, USA) without cooling at the midshaft of the femoral bone. Fracture fragments were contacted and stabilized, and the intramedullary was then fixed using a stainless-steel wire (diameter, 1.4 mm). The wire was cut on the surface of the intercondylar groove to avoid restriction of knee joint motion. The fascial and skin incisions were closed with a 3-0 nylon suture. During surgery, a mixture of medetomidine + midazolam + butorphanol was used for the anesthesia; medetomidine and butorphanol have strong analgesic effects. The rats were housed in separate cages, given food and water *ad libitum*, and their conditions were monitored daily.

Study groups

A total of 40 operated Sprague–Dawley rats were divided into four groups: the control group (C group; n = 10; administered saline), the romosozumab group (R group; n = 10; administered romosozumab, 25 mg/kg), the vitamin D_3 group (VD group; n = 10; administered active vitamin D_3, 0.2 μg/kg), and the romosozumab plus vitamin D_3 group (R + VD group; n = 10; administered romosozumab plus vitamin

D_3). Romosozumab (Amgen Inc, Japan, Tokyo) was administered once a month and active vitamin D_3 (Rocaltrol, Kyowakirin, Inc, Japan, Tokyo) was administered twice a week. In addition, a sham-operated group (n = 10) was prepared, but the group was not analyzed statistically with the other four groups. The study design is shown in Fig. 1.

Harvesting of femurs and blood

Ten weeks after femoral osteotomy, 0.15 mg/kg medetomidine hydrochloride + 2.0 mg/kg midazolam + 2.5 mg/kg butorphanol was injected into the peritoneum, and cervical dislocation was performed. The operated right femoral bones were explanted, and the right bones were separated from the stainless-steel wire before analysis. We used the left femoral bones, which had not been operated upon, to evaluate the effect of the combined treatment of romosozumab with active vitamin D_3 on the bones of OVX rats using microcomputed tomography (micro-CT) analysis.

Soft X-ray analysis

The right femoral bones obtained at the 10-week time point were photographed using Softex X-ray apparatus (Softex CSM-2; Softex, Tokyo, Japan) with HS Fuji Softex film (Fuji Film, Tokyo, Japan) at 45 cm, 30 kV, and 15 mA for 20 s. The fusion was quantified using the anteroposterior (A–P) and lateral radiographs. Three independent, blinded observers scored the bone formation in each rat using a four-point scale. Fracture union was judged by visual assessment of the mineralized callus bridging the fracture line on the A–P radiographs (right side: 1 point; left side: 1 point) and lateral radiographs (anterior side: 1 point; posterior side: 1 point). The bone fusion was considered to be >2 points with soft X-ray images on a four-point scale. In addition, the Radiographic Union Scale in Tibial Fractures (RUST) was used to assess all specimens. The RUST score is based on the presence or absence of a callus and of a visible fracture line at a total of four cortices visible on the A–P and lateral radiographs, and its four-point minimum corresponds to a fracture that is deemed not healed, whereas its 12-point maximum corresponds to a fracture that is deemed healed with all cortices bridged with a callus, without a fracture line. Kooistra et al. reported the reliability and validity of the RUST scale in human long bone[13].

Histopathological analysis

After the specimens were harvested, they were dissected until they were free of soft tissue. They were then immersed in 70% ethanol for 1 day and in 99.5% ethanol for 1 day. The bones were then sequentially immersed in acetone for 1 day, in 99.5% ethanol for 1 day, and in 2-propanol for 1 day. The next day, the bones were embedded in glycolmethacrylate, without previous decalcification, and left to stand for 10 days. Using a fully automated rotary microtome (Leica RM2255, Leica, Nussloch, Germany), the femurs were cut into 3-μm thick sections, and the specimen was stained with toluidine blue.

Fracture bone micro-CT analysis (operated side)

The bone micro-CT imaging was performed according to the guidelines[14]. The explanted femoral bones were scanned using a Sky-Scan 1172 tomograph (Bruker micro-CT, Kontich, Belgium) with a voxel size of 20 mm. Data were collected at 100 kV and 100 mA and reconstructed using the cone-beam algorithm. Each femoral bone was set on the object stage, and sample scanning was performed over 180° of rotation with an exposure time of 105 ms. A cylindrical volume of interest with a diameter of 20 mm and a height of 27 mm was selected, which displayed the microstructure of the rat femoral bones (comprising the cortical and trabecular bones). Data analysis was performed using CT Analyzer software (Bruker micro-CT). The region of interest was set as the area of fracture healing and was defined by the fracture area filled with new bone; the structural indices of the femoral fracture areas (9 × 9 × 8.4 mm; a fracture gap in the center) were calculated using this software. During the three-dimensional analysis, the bone volume/tissue volume (BV/TV), the BV of cortical bone, the TV, the trabecular thickness (Tb. Th), the trabecular number (Tb. N), and the trabecular separation (Tb. Sp) were measured.

Bone micro-CT analysis (nonoperated side)

The bone micro-CT imaging was performed according to the guidelines [14]. The explanted femoral bones were scanned using a Sky-Scan 1172 tomograph (Bruker micro = CT, Kontich, Belgium) with a voxel size of 20 mm. Data were collected at 100 kV and 100 mA and reconstructed using the cone-beam algorithm. Each femoral bone was fixed in a sample holder and set with the vertical axis on the object stage, and sample scanning was performed over 180° of rotation with an exposure time of 105 ms. A cylindrical volume of interest with a diameter of 20 mm and a height of 27 mm was selected, which displayed the microstructure of the rat femoral bones (comprising the cortical and trabecular bones). Data analysis was performed using CT Analyzer software (Bruker micro-CT). The region of interest was set at the distal femoral area, and the structural indices of the femoral area of trabecular bone analysis (0.8–3.8 mm) from the growth-plate reference level and the area of cortical bone analysis (3.0–3.8 mm) from the growth-plate reference level were calculated using this software. During the three-dimensional analysis, the BV/TV, the BV of trabecular bone, the TV, the Tb. Th, the Tb. N, the Tb. Sp, the BV of cortical bone, the cortical bone area (Cr. Ar), and the cortical bone thickness (Cr. Th) were measured.

Biomechanical analysis

Nonfractured femurs were used to test the bone strength. Three-point bending tests were conducted using a universal material testing system (Instron 5865; Instron, Kanagawa, Japan). The femur was placed on the sample support with its anterior surface facing upward and the center of the femoral shaft located at the center of the support. The load was applied at a rate of 1 mm/s until the bone was fractured. A program prepared by Instron was used for data analysis; the measured parameters were the maximum load, maximum bending stress, stiffness, Young’s modulus, and toughness.

Measurement of serum levels of bone turnover markers

Blood samples (100 μL) were collected when the animals were euthanized at week 10. Serum levels of osteocalcin (OC), an osteogenesis marker, were measured with a Rat Osteocalcin enzyme-linked

immunosorbent assay (ELISA) Kit (RK03858, Woburn, MA). Cross-linked C-telopeptides of type-1 collagen (CTX-1), a bone-resorption marker, were measured using the Rat Cross-linked C-telopeptide of Type-1 Collagen ELISA Kit (RK03603, Woburn, MA).

Statistical methods

Statistical analysis of the four groups, but not the sham group, was performed. Normality was confirmed by the Shapiro–Wilk test. Variables that were normative were subjected to one-way analysis of variance to compare the differences between the four groups. One-way analysis of variance with the Bonferroni posthoc test was used for the four-point test results, RUST, morphometric analysis, biomechanical analysis, and bone turnover marker analysis. For the four-point test and RUST, kappa statistics were performed to check for interobserver variability. The kappa statistic corrects the observed agreement for a possible chance agreement among observers. Agreement was rated as follows: poor, $\kappa = 0–0.20$; fair, $\kappa = 0.21–0.40$; moderate, $\kappa = 0.41–0.60$; substantial, $\kappa = 0.61–0.80$; excellent, $\kappa > 0.81$. A value of 1 indicated absolute agreement, whereas a value of 0 indicated agreement no better than chance. All analyses were performed using Statistical Package for the Social Sciences software (SPSS V25.0; IBM SPSS Statistics for Windows, IBM Corp., Armonk, NY). Statistical significance was set at $p < 0.05$.

Results

X-ray imaging: combination therapy had no effect on bone healing

On soft X-ray imaging of femurs harvested at week 10, fracture lines were unclear in the R, VD, and R + VD groups, and abundant callus formation was observed in the R and R + VD groups. In contrast, fracture lines were clear in the C group. Consistent agreement ($\kappa = 0.88$) was found among the three independent observers who scored the radiographs. On the four-point scale, the C group scored 0.7 ± 0.8 points, the R group scored 0.4 ± 0.5 points, the VD group scored 1.3 ± 1.9 points, and the R + VD group scored 2.3 ± 1.6 points; there were no significant differences in the scores between the groups. On the RUST scale, the C group scored 8.0 ± 0.8 points, the R group scored 7.4 ± 1.3 points, the VD group scored 6.7 ± 1.3 points, and the R + VD group scored 7.9 ± 0.9 points; there were no significant differences in the scores between the groups. (Table 1).

Toluidine blue staining in nondecalcified specimens showed mature bridge formation without endochondral ossification in the R and R + VD groups

The results of bone histopathological analyses with toluidine blue staining revealed abundant immature callus formation and endochondral ossification in the sham and control groups. However, mature bridges were formed without endochondral ossification in the R and R + VD groups (Fig. 2).

After combined therapy, micro-CT examination of the operated side showed no differentiation of each parameter improved

The micro-CT examination results on the operated side are shown in Fig. 3. After the combined therapy, the microstructure parameters of the R + VD group were lower than that of the R group. The BV/TV and BV of trabecular bone were significantly higher in the R group than in the VD and R + VD groups ($p < 0.01$, $p < 0.05$). In contrast, the BV/TV, BV values of trabecular bone, and the TV, Tb. Th, Tb. N, and Tb. Sp values in the R and R + VD groups were not significantly different from those in the C group.

After combined therapy, micro-CT examination of the nonoperated side showed absolute improvement in trabecular BV

The micro-CT examination results for the nonoperated side are shown in Fig. 4. The BV/TV and BV values of the trabecular bone were significantly higher in the R and R + VD groups than in the C group ($p < 0.05$, $p < 0.01$). Compared with the C group, significant differences in the Tb. Th and Tb. N values were observed in the R and R + VD groups, showing increases in the Tb. Th and Tb. N values and a decrease in the Tb. Sp value. No significant differences in cortical bone among the groups were observed (Table 2).

The three-point bending test showed that combined therapy increased bone strength

The three-point bending test results are presented in Fig. 5. The values of maximum bending stress, stiffness, and Young's modulus were higher in the order of R + VD group > R group > C group. The values of maximum load and toughness were higher in the order of R group > R + VD group > C group.

Bone turnover markers were comparable between groups

The OC and CTX-1 measurement results are presented in Table 3. No significant differences in the OC and CTX-1 serum levels were noted between the groups.

Discussion

The results of evaluation on the operated side showed that combination therapy with romosozumab and active vitamin D_3 did not produce an increase in callus mass or continuity of the cortical bone. Previous experimental reports of romosozumab in rats have used a dose of romosozumab that is higher than a conversion dose for humans, and it is unclear whether previous studies have been able to show the true effects of romosozumab. Therefore, in the present experiment, the dose was 25 mg/kg once a month. The results from the nonfracture side proved that romosozumab was sufficiently effective at that dose. Suen et al. showed that treatment with romosozumab (25 mg/kg, twice a week) significantly increased newly formed blood vessels in a rat fracture model[8]. Gao et al. showed that treatment with romosozumab (25 mg/kg, twice a week) increased the level of bone morphogenetic protein-2, a bone morphogenetic factor, in an 8-week-old OVX rat fracture model[7]. The findings from these reports imply that romosozumab has a bone union-promoting effect. However, Morse et al. reported that romosozumab treatment (25 mg/kg biweekly) increased the callus mass and bone strength but did not increase the bone union rate in a rat fracture model[9]. This is consistent with our results. In addition, there are a

handful of reports of acceleration of bone fracture healing with romosozumab in humans in which the results showed that there was no effect[15][16].

The micro-CT imaging results for the femur on the nonfractured side demonstrated that romosozumab treatment improved the microstructure of the trabecular bone. Increases in trabecular bone mass, Tb. Th, and Tb. N on the nonfractured side were found in the rats that received combination therapy of romosozumab and active vitamin D_3, confirming that the morphological changes were equivalent to or greater than those obtained with romosozumab alone. There are some reports that romosozumab treatment in OVX models indicates bone anabolic effects[17][18], especially improvement of the loss of cancellous bone. The micro-CT results on the nonfracture side showed that the effect of romosozumab plus vitamin D_3 was equal to or superior to that of romosozumab alone. However, the micro-CT results for the fracture side, including BV/TV and trabecular bone BV, showed there was no advantage of the combination therapy over romosozumab alone. Although the cause is unknown, it was suggested that the combination with romosozumab may not have a cooperative effect on the fracture side. In OVX rats, the administration of active vitamin D_3 has been reported to significantly decrease the number of osteoclasts in bone tissue and affect osteoblast differentiation and remodeling[19]. Furthermore, a study using a bone-resorption inhibitor and active vitamin D_3 showed that this combination decreased the blood parathyroid hormone level[20]. These previous reports suggested that combination therapy with romosozumab and active vitamin D_3 caused morphological improvements in the trabecular BV by means of a bone-remodeling-promoting effect, and reduced bone resorption due to decreased blood parathyroid hormone levels.

Regarding bone turnover, a study in humans showed that increases in bone-formation marker levels and decreases in bone-resorption marker levels peaked on day 14 after romosozumab administration[21]. No such differences were observed in our study presumably because the bone turnover marker levels were measured only when the animals were euthanized at week 10.

There were several limitations to this study. For example, the progress of fracture healing was not followed over time by radiography and bone turnover marker levels. Preliminary studies showed no change in the course of treatment of fractures by X-ray and no difference in bone metabolic markers.

Conclusions

Combination therapy with romosozumab and active vitamin D_3 was administered to an OVX rat fracture model. The results indicated that the combination therapy improved trabecular BV but did not contribute to accelerated fracture healing. It appears that accelerated fracture healing does not occur with romosozumab alone or with romosozumab in combination with active vitamin D_3.

Abbreviations

OVX Ovariectomize

RUST Radiographic union scale in tibial fractures

BV/TV Bone volume/tissue volume

Tb.Th Trabecular thickness

Tb.N Trabecular number

Tb.Sp Trabecular separation

Cr.Ar Cortical bone area

Cr.Th Cortical bone thickness

OC Osteocalcin

CTX-1 Cross-linked C-telopeptides of type-1 collagen

ELISA Enzyme-linked immunosorbent assay

R Romosozumab

VD Active vitamin D_3

Declarations

Ethics approval and consent to participate

This study was conducted in accordance with the Declaration of Helsinki. Approval was obtained from the Oita University animal research committee prior to animal experimentation (Oita University institutional Animal Ethics Committee no. 182402)

Consent for publication

Not applicable

Availability of data and material

All data generated or analyzed during this study are included in this published article.

Competing interest

The authors declare that they have no competing interests.

Funding

This work was supported by JSPS KAKENHI Grant Number 21K09302.

Author contributions

RT, TI, YT, TK, and MK carried out the operation. HT conceived of the study design. RT, TO, TI, YT, TK, MK and HT interpreted the data and drafted the manuscript. All authors read and approved the final manuscript.

Acknowledgements

We are grateful to Miss Shiba Fumiko and Oshima Minori for excellent technical assistance.

References

1. Zura R, Watson JT, Einhorn T, Mehta S, Della Rocca GJ, Xiong Z, et al. An inception cohort analysis to predict nonunion in tibia and 17 other fracture locations. Injury. 2017;48:1194–203.
2. Zura R, Xiong Z, Einhorn T, Watson JT, Ostrum RF, Prayson MJ, et al. Epidemiology of fracture nonunion in 18 human bones. JAMA Surg. 2016;151:1–12.
3. Buza J. Bone healing in 2016. Clin Cases Miner Bone Metab [Internet]. 2016;13:101–5.
4. Hak DJ, Fitzpatrick D, Bishop JA, Marsh JL, Tilp S, Schnettler R, et al. Delayed union and nonunions: Epidemiology, clinical issues, and financial aspects. Injury. 2014;45:S3–7.
5. Liu Y, Rui Y, Yan Cheng T, Huang S, Xu L, Meng F, et al. Effects of Sclerostin Antibody on the Healing of Femoral Fractures in Ovariectomised Rats. calcif tissue int. 2016;98:263–74.
6. Ominsky MS, Niu QT, Li C, Li X, Ke HZ. Tissue-level mechanisms responsible for the increase in bone formation and bone volume by sclerostin antibody. J Bone Miner Res. 2014;29:1424–30.
7. Feng G, Chang-Qing Z, Yi-Min C, Li X-L. Systemic administration of sclerostin monoclonal antibody accelerates fracture healing in the femoral osteotomy model of young rats. Int Immunopharmacol. 2014;24:7–13.
8. Suen PK, He YX, Chow DHK, Huang L, Li C, Ke HZ, et al. Sclerostin monoclonal antibody enhanced bone fracture healing in an open osteotomy model in rats. J Orthop Res. John Wiley and Sons Inc.; 2014;32:997–1005.
9. Morse A, Mcdonald MM, Schindeler A, Peacock L, Mikulec K, Cheng TL, et al. Sclerostin Antibody Increases Callus Size and Strength but does not Improve Fracture Union in a Challenged Open Rat Fracture Model. 2017;101:217–28.
10. Roberts JL, Drissi H. Advances and Promises of Nutritional Influences on Natural Bone Repair. J Orthop Res. 2020;38:695–707.
11. Fischer V, Haffner-Luntzer M, Prystaz K, Vom Scheidt A, Busse B, Schinke T, et al. Calcium and vitamin-D deficiency marginally impairs fracture healing but aggravates posttraumatic bone loss in osteoporotic mice. Sci Rep. 2017;7:7223.

12. Tsubouchi Y, Ikeda S, Kataoka M, Tsumura H. Combination therapy with low-dose teriparatide and zoledronate contributes to fracture healing on rat femoral fracture model.J Orthop Surg Res. 2018;13:267.
13. Kooistra BW, Dijkman BG, Busse JW, Sprague S, Schemitsch EH, Bhandari M. The radiographic union scale in tibial fractures: Reliability and validity. J Orthop Trauma. 2010;24:81–6.
14. Bouxsein ML, Boyd SK, Christiansen BA, Guldberg RE, Jepsen KJ, Müller R. Guidelines for assessment of bone microstructure in rodents using micro-computed tomography. J Bone Miner Res. 2010;25:1468–86.
15. Schemitsch EH, Miclau T, Karachalios T, Nowak LL, Sancheti P, Poolman RW, et al. A Randomized, Placebo-Controlled Study of Romosozumab for the Treatment of Hip Fractures. J Bone Joint Surg Br. 2020;102:693–702.
16. Bhandari M, Schemitsch EH, Karachalios T, Sancheti P, Poolman RW, Caminis J, et al. Romosozumab in Skeletally Mature Adults with a Fresh Unilateral Tibial Diaphyseal Fracture: A Randomized Phase-2 Study. J Bone Joint Surg Am. 2020;102:1416–26.
17. Suen PK, Zhu TY, Ho D, Chow K, Huang L, Zheng L-Z, et al. Sclerostin Antibody Treatment Increases Bone Formation, Bone Mass, and Bone Strength of Intact Bones in Adult Male Rats OPEN. Nat Publ Gr. 2015;23:1–9.
18. Ma YL, Hamang M, Lucchesi J, Bivi N, Zeng Q, Adrian MD, et al. Time course of disassociation of bone formation signals with bone mass and bone strength in sclerostin antibody treated ovariectomized rats. Bone. 2017;97:20–8.
19. de Freitas PHL, Hasegawa T, Takeda S, Sasaki M, Tabata C, Oda K, et al. Eldecalcitol, a second-generation vitamin D analog, drives bone minimodeling and reduces osteoclastic number in trabecular bone of ovariectomized rats. Bone. 2011;49:335–42.
20. Ebina K, Kashii M, Hirao M, Hashimoto J, Noguchi T, Koizumi K, et al. Comparison of the effects of denosumab between a native vitamin D combination and an active vitamin D combination in patients with postmenopausal osteoporosis. J Bone Miner Metab. Springer Japan; 2017;35:571–80.
21. Cosman F, Crittenden DB, Adachi JD, Binkley N, Czerwinski E, Ferrari S, et al. Romosozumab Treatment in Postmenopausal Women with Osteoporosis. N Engl J Med. 2016;375:1532–43.

Tables

Table 1. Results of bone radiographic findings of rat femur and radiographic statistical analysis

	Sham	C	R	VD	R+VD
			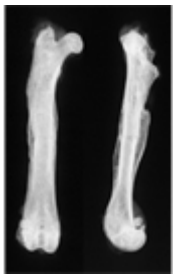		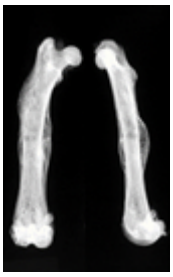
4-point scale (point)	0.75±1.5	0.7±0.8	0.4±0.5	1.3±1.9	2.3±1.6
RUST (point)	8.4±1.4	8.0±1.0	7.4±1.3	6.7±1.3	7.9±0.9

Sham: sham group, C: control group, R: romosozumab group, VD: active vitamin D_3 group, R + VD: romosozumab + active vitamin D_3 group. The fracture line was clear in the C group. On the other hand, fracture lines were unclear in the R group, VD group, and R + VD group, whereas abundant callus formation was observed for the R and R + VD groups. No significant differences were observed in the four-point test and RUST scores between the groups.

Table 2. Results of cortical bone morphometrical analysis for the nonoperated side.

	Sham	C	R	VD	R+VD
	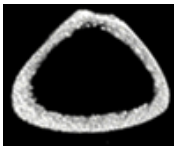	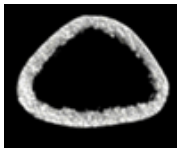	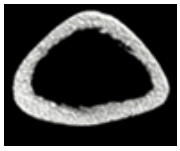		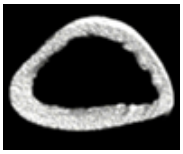
BV of cortical bone (mm3)	4.65±0.46	4.87±0.25	5.05±0.26	4.65±0.34	5.15±0.39
Cr.Ar (mm2)	5.68±0.56	5.96±0.30	6.18±0.32	5.69±0.42	6.29±0.48
Cr.Th (mm)	0.36±0.04	0.36±0.02	0.39±0.03	0.34±0.03	0.38±0.04

Sham: sham group, C: control group, R: romosozumab group, VD: active vitamin D_3 group, R + VD: romosozumab + active vitamin D_3 group. Cr. Ar: cortical bone area, Cr. Th: cortical bone thickness. All parameters were increased more in the R and R + VD groups compared to in the C group, but no significant differences in BV of cortical bone, cortical bone area and cortical bone thickness between the groups were observed.

Table 3. Results of serum bone turnover marker level analysis.

	Sham	C	R	VD	R+VD
OC (pg/mL)	126.29±45.94	110.15±51.33	111.76±25.13	136.30±55.66	175.28±125.34
CTX-1 (pg/mL)	443.97±69.31	471.74±56.94	473.94±51.30	478.47±44.61	456.92±53.79

Sham: sham group, C: control group, R: romosozumab group, VD: active vitamin D_3 group, R + VD: romosozumab + active vitamin D_3 group. OC: osteocalcin, CTX-1: Cross-linked C-telopeptide of type-1 collagen. Osteocalcin (OC) showed bone-formation activity, and cross-linked C-telopeptide of type-1 collagen (CTX-1) showed bone-resorption activity. The OC values were higher in the VD and R + VD groups compared to the C group. The CTX-1 values in every group were similar. No significant differences in the serum levels of OC and CTX-1 were noted between the groups.

Figures

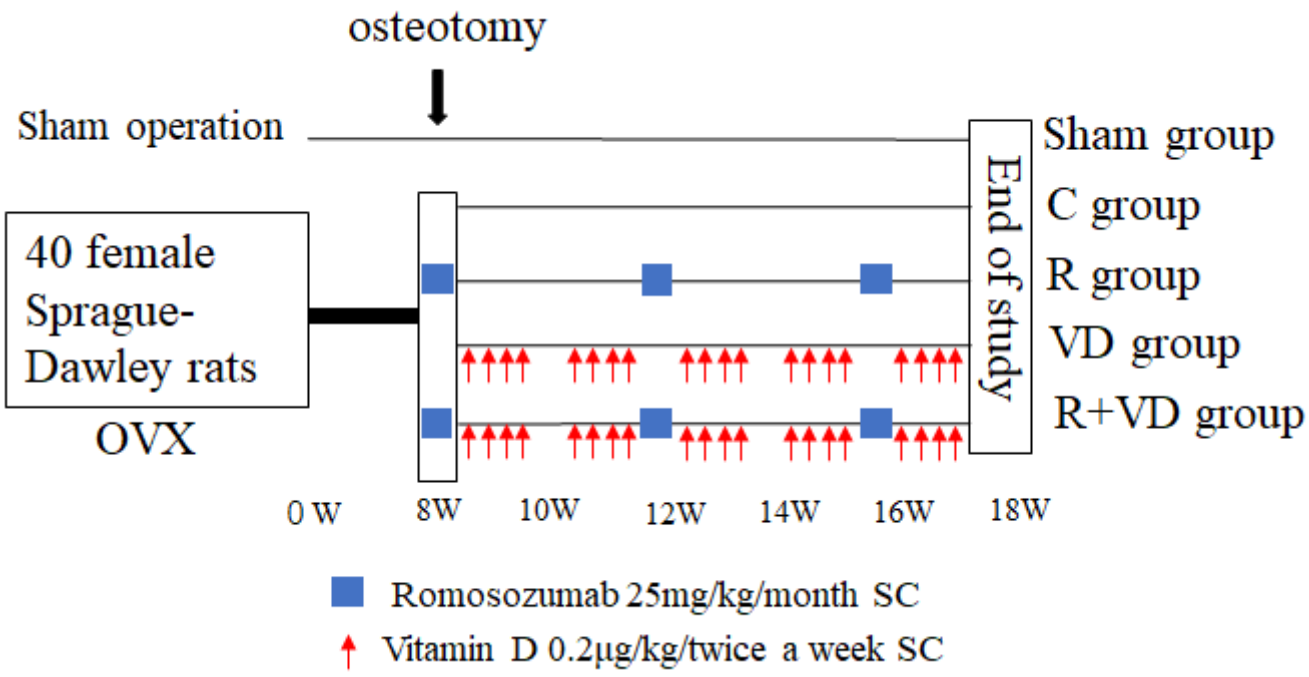

Figure 1

Study and administration schema

Control group (C: administered saline), romosozumab group (injected subcutaneously 25 mg/kg/once a month), vitamin D_3 group (VD: injected subcutaneously 0.2 μg/kg/twice a week), R + VD group. Following ovariectomy of female Sprague–Dawley rats (aged 24 weeks), rats were divided into four groups (n = 10 in each group). After 8 weeks, femoral osteotomy was performed. At 18 weeks, rats were sacrificed, and both femoral bone and blood were taken.

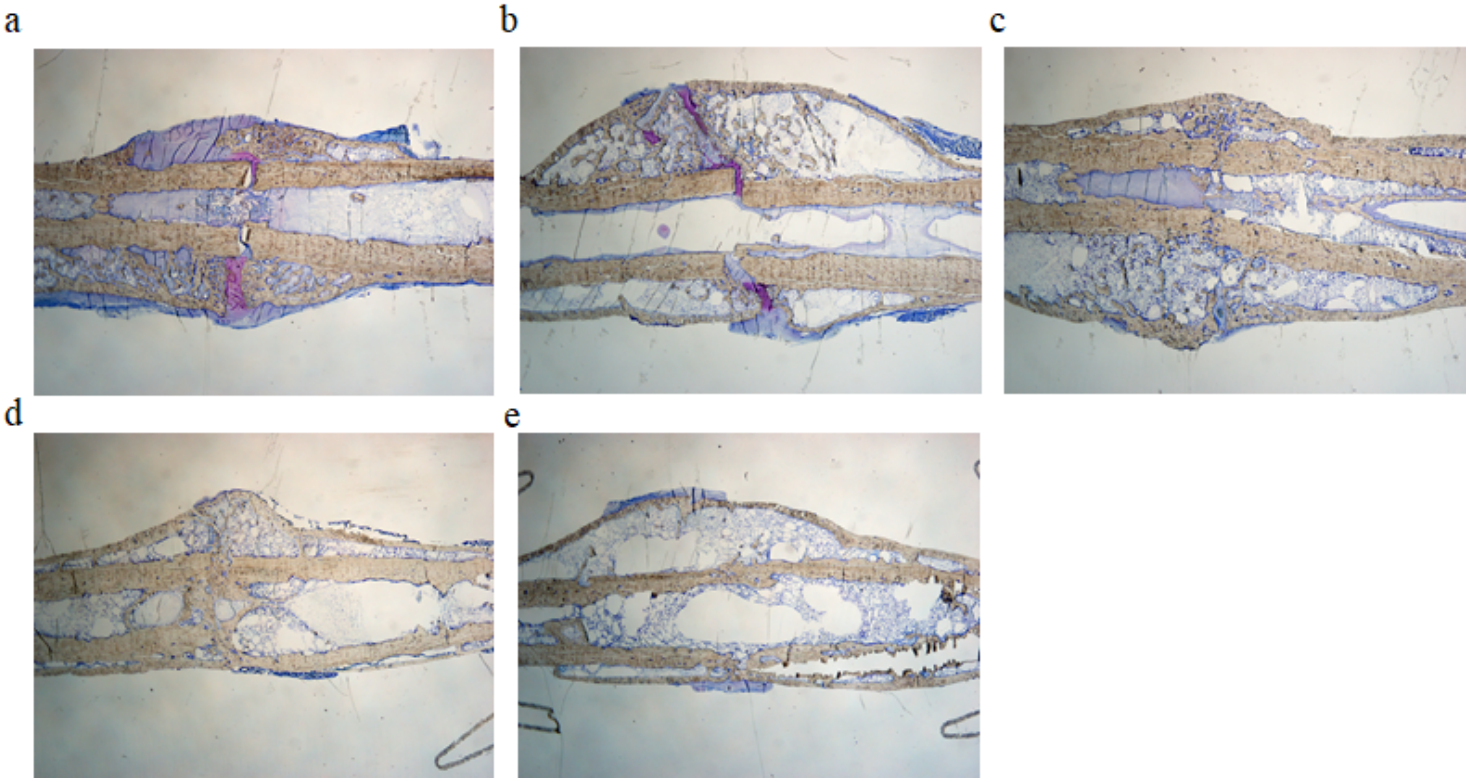

Figure 2

Results of bone histological findings of nondemineralized specimens for rat femurs (toluidine blue staining, ×1). a) Sham group, b) C group, c) R group, d) VD group, e) R + VD group. Toluidine blue staining revealed many immature callus formations and endochondral ossifications in the sham and C groups. However, mature bridges were formed without endochondral ossification in the R and R + VD groups.

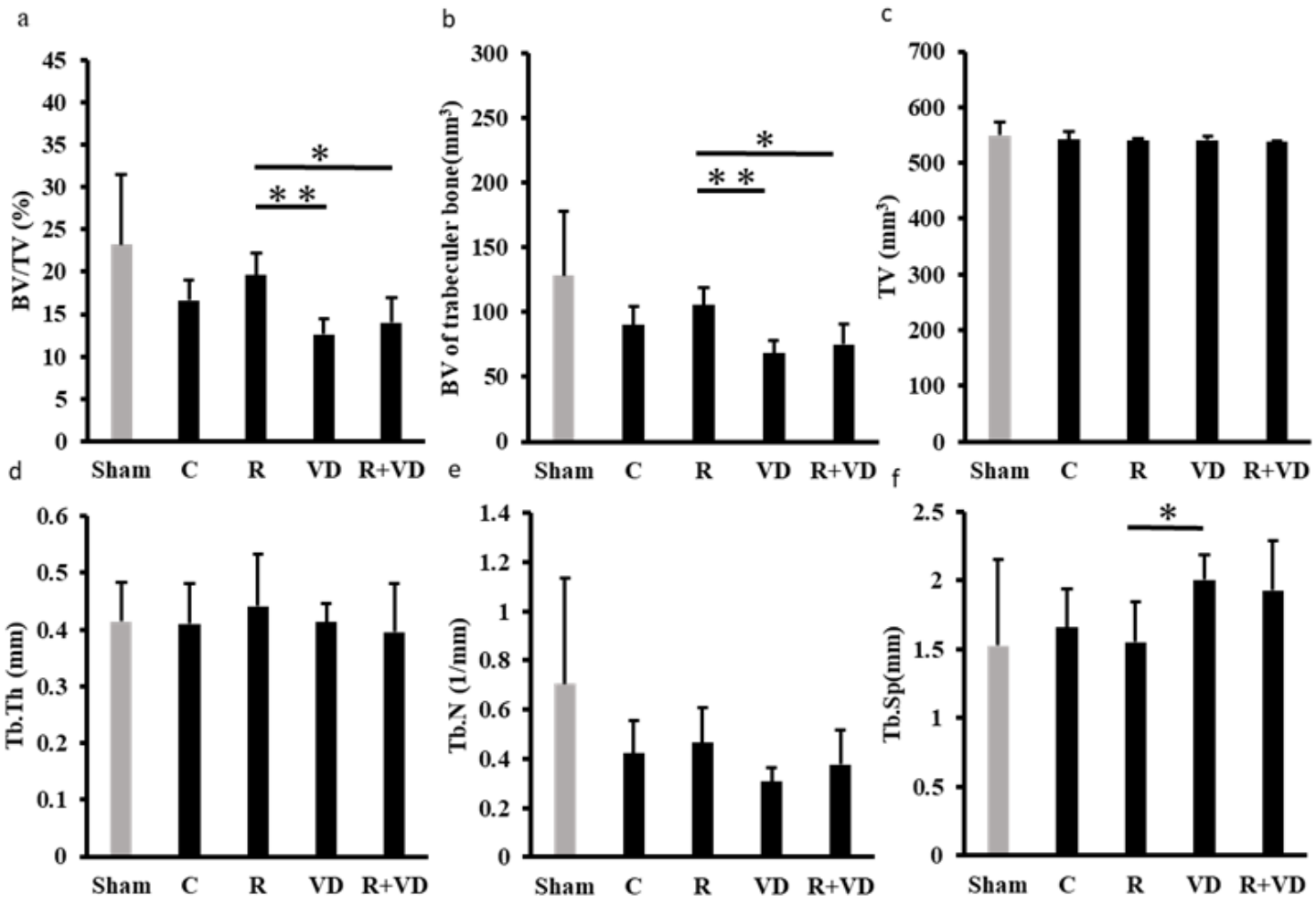

Figure 3

Results of bone morphometrical analysis for operated side. a) Bone volume/tissue volume (BV/TV), b) BV of trabecular bone, c) TV, d) trabecular thickness (Tb. Th), e) trabecular number (Tb. N), f) trabecular separation (Tb. Sp).

The results of the morphological analysis of the femur on the fracture side are shown. The BV value of the trabecular bone in the R group was significantly higher than that in the VD group or the R + VD group ($p < 0.01$, $p < 0.05$). The Tb. Sp value in the VD group was significantly higher than that in the R group ($p < 0.01$).

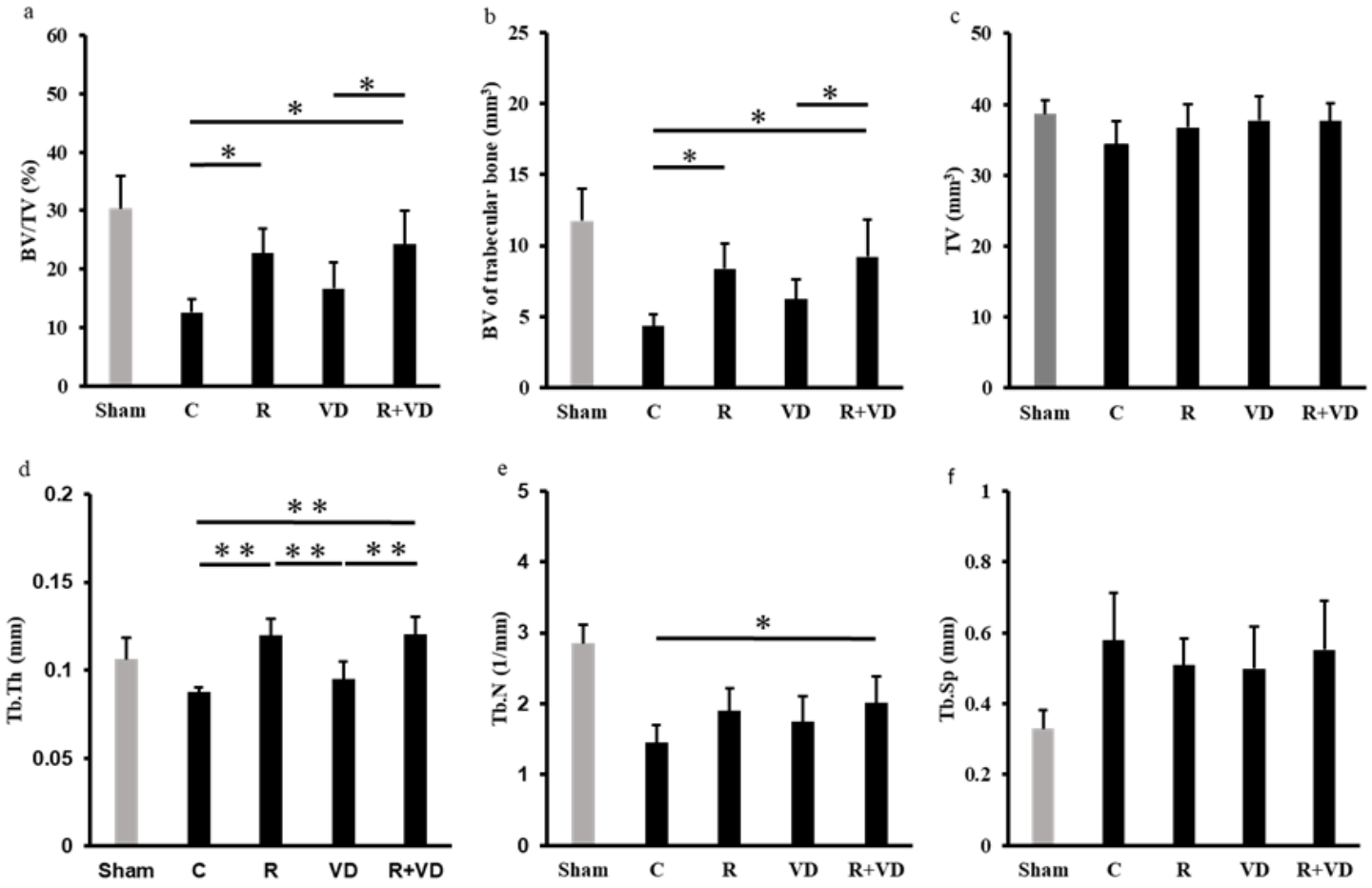

Figure 4

Results of trabecular bone morphometrical analysis of the nonoperated side. a) BV/TV: Bone volume/tissue volume, b) BV of trabecular bone, c) TV, d) Tb. Th: trabecular thickness, e) Tb. N: trabecular number, f) Tb. Sp: trabecular separation. The BV/TV and BV values of the trabecular bone were significantly higher in the R and R + VD groups than in the C group ($p < 0.05$, $p < 0.01$). The Tb. Th and Tb. N values were significantly higher in the R and R + VD groups than in the C group.

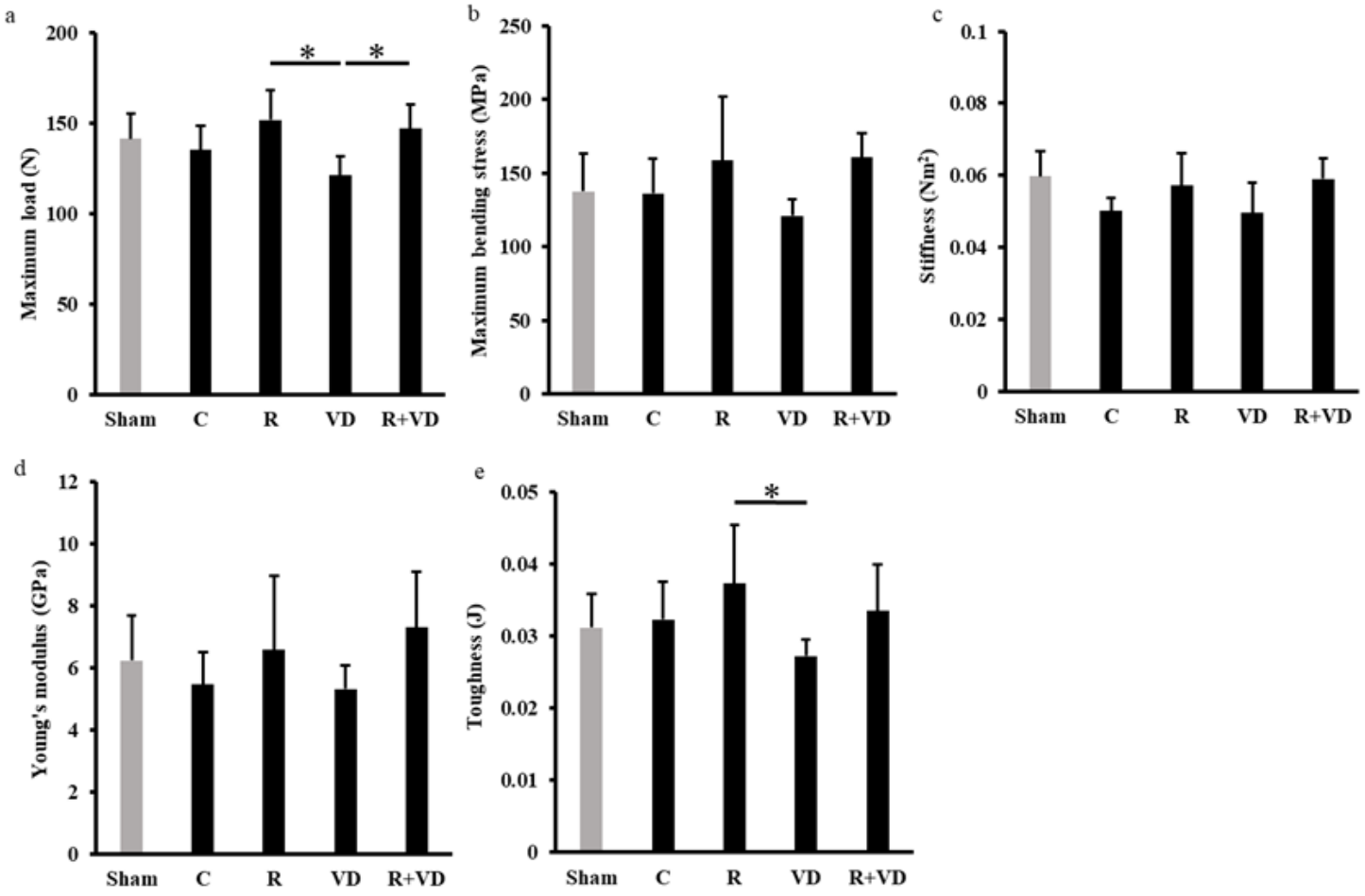

Figure 5

Results of biomechanical analysis for the nonoperated side. a) Maximum load, b) maximum bending stress, c) stiffness, d) Young's modulus, e) toughness. The values of maximum bending stress, stiffness, and Young's modulus were higher in the order of R + VD group > R group > C group. The values of maximum load and toughness were higher in the order of R group > R + VD group > C group.